

Effect of post-weld heat treatment on microstructure and properties of Ti-23Al-17Nb alloy laser beam welding joints

WANG Guo-qing(王国庆), WU Ai-ping(吴爱萍), ZHAO Yue(赵 玥),
ZOU Gui-sheng(邹贵生), CHEN Qiang(陈 强), REN Jia-lie(任家烈)

Key Laboratory for Advanced Materials Processing Technology of the Ministry of Education,
Department of Mechanical Engineering, Tsinghua University, Beijing 100084, China

Received 12 May 2009; accepted 23 July 2009

Abstract: The mechanical properties of Ti-23Al-17Nb (mole fraction, %) laser beam welding alloy joint at room temperature are comparable to that of the base materials. However, the strength and ductility of the as-welded joint deteriorate seriously after high temperature circulation. The effect of post-welded heat treatment on the microstructure and mechanical properties of the joint was investigated. The heat treatment was taken at 980 °C for 1.5 h, then furnace cooling and air cooling were performed separately. The results indicate that proper post-welded heat treatment improves the ductility of the joint at high temperature.

Key words: Ti-23Al-17Nb; Ti₃Al-based alloy; laser beam welding; post-weld heat treatment; mechanical properties

1 Introduction

Ti-23Al-17Nb is one of the well developed Ti₃Al-based alloys in China[1–4], and one of the most competitive candidates as the high temperature structural materials used in space and aerospace fields[5]. Welding is an indispensable processing method in its application. Although there were some research works on the weldability, fusion welding and brazing of Ti₃Al alloy[6–17], these works mainly focused on as-welded microstructure and room-temperature properties (mainly room-temperature tensile properties) of welding joints. Because of their high energy density, laser beam (LB) welding and electron beam (EB) welding have narrow weld zone and heat-affected zone (HAZ), and the microstructure coarsening problem of traditional arc welding also could be improved by these two welding methods. Therefore, they are preferable methods in fusion welding for Ti₃Al intermetallic compound. In welding joints, under the conditions of laser beam welding and electron beam welding, the weld metal and the fields above the transition temperature in the HAZ were mainly composed of unstable β/B_2 phase. When the transverse tensile tests of the joints were conducted, because of the narrow weld metal zone and HAZ as well

as the columnar crystal grain in the weld metal, the deformation mainly took place in base metal zone. The joints' transverse tensile strength was comparable to that of the base metal, and its ductility achieved around 70% of that of the base metal, but its bend ductility was lower. When the bending strain achieved 1%–4%, cracks started to occur in the weld metal[6]. Moreover, because β/B_2 phase in the joints was unstable, it would transform to adverse microstructure, leading to serious deterioration of high-temperature properties and room-temperature properties after high temperature circulation[18]. It is necessary to adjust unstable microstructure of the as-welded joints. The post-weld heat treatment is one of the methods which could adjust microstructure and properties of the joints. In this work the effect of heat treatment on microstructure and properties of Ti-23Al-17Nb alloy laser beam welding joints was studied.

2 Experimental

The experimental materials provided by China Iron and Steel Research Institute(CISRI) were prepared by the following steps: vacuum-consumable electrode arc-melting, breaking down in the β/B_2 phase fields, forging in the α_2+B_2 phase field, rolling in α_2+B_2+O phase field,

heat treatment at 980 °C for 1 h, followed by air-cooling. The sheet was 400 mm long, 160 mm wide and 3 mm thick. The long direction was along the rolling direction. The microstructures of the rolling surface and longitudinal section of the base metal with XRD analysis results are shown in Fig.1. The chemical compositions and mechanical properties are listed in Table 1 and Table 2, respectively.

The oxide layers were removed from the surfaces by mechanical polishing and the specimens were cleaned with acetone and absolute alcohol, and then dried. The weld was perpendicular to the rolling direction. The laser beam welding was performed by a fast axial flow type CO₂ laser PRC-3000 with lens focus of 190 mm; two sets of welding parameters were applied, the output power and the welding speed of which were 2 000 W, 1.5 m/min and 2 500 W, 1.875 m/min, respectively. The nominal heat inputs were all 800 J/cm. The focal point was on the surface of the specimens and flowing helium (99.995% purity) shielding from both top and back sides along the whole bead was used during welding. Full penetration welds with perfect appearance were obtained. The appearance of the welded joint is shown in Fig.2 and the macrostructure of the cross-section is shown in Fig.3.

In order to reserve the properties of base material and improve the microstructure of the welds, the heat treatment temperature was set at 980 °C at a heating rate

of 0.133 °C/min. The holding time was 1.5 h. Then furnace cooling and air cooling were performed separately. Argon was used for shielding during heating and furnace cooling.

The dimensions of the tensile specimens are shown in Fig.4. The weld specimens were prepared with wire-electrode cutting and then ground. Tensile tests at room temperature were carried out according to Chinese Standard GB/T228 — 2002. Tensile tests at high temperature were carried out according to Chinese Standard GB/T4338—1995 at 650 °C. Four specimens were tested under each condition.

The microstructure of the joints' cross-section was investigated by an optical microscope. The specimens

Table 1 Chemical compositions of experimental materials (mass fraction)

Nb	Al	O	N	H	Ti
30.62	12.98	0.054	0.004	0.0012	Balance

Table 2 Main mechanical properties of Ti₃Al alloy along rolling direction

Temperature	σ_b /MPa	$\sigma_{0.2}$ /MPa	δ /%
Room temperature	893.30	693.30	40.00
High temperature (650 °C)	837.50	—	16.75

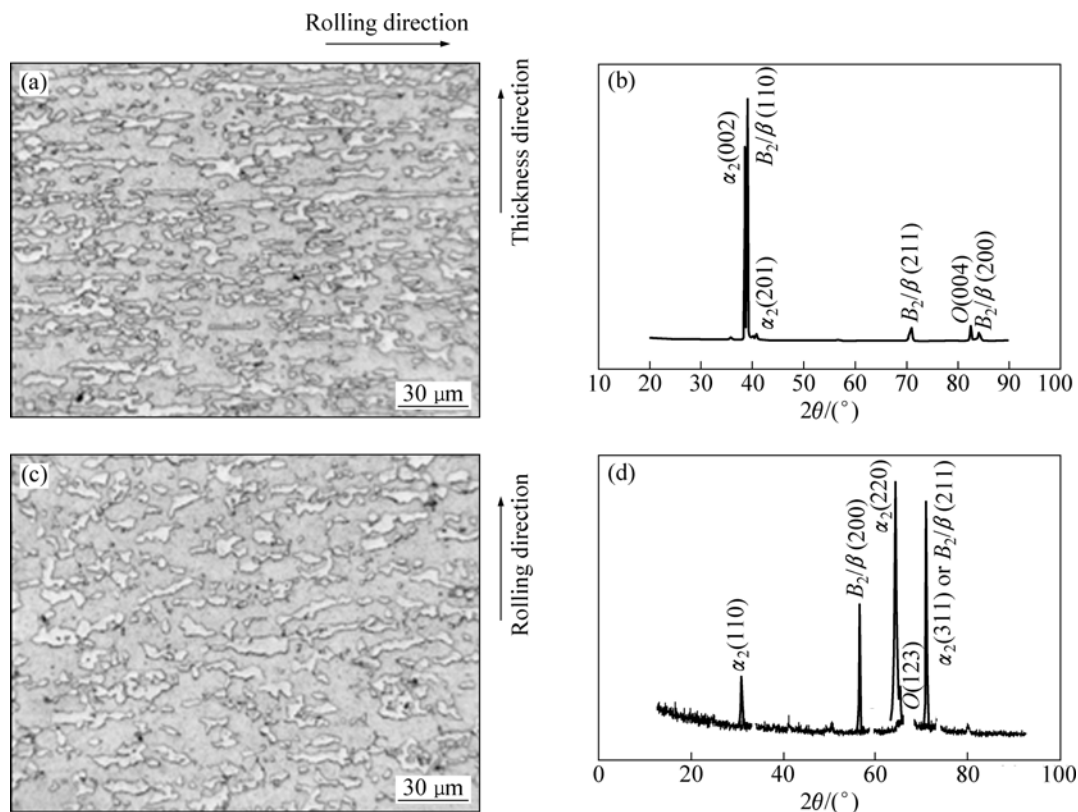


Fig.1 Optical images and XRD patterns of base metal: (a) Microstructure of longitudinal section; (b) XRD pattern of longitudinal section; (c) Microstructure along with rolling surface; (d) XRD pattern along rolling surface

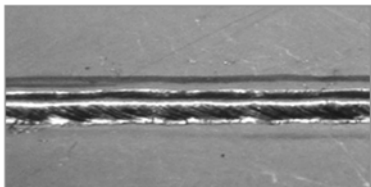
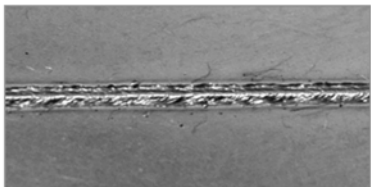
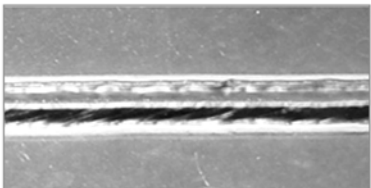
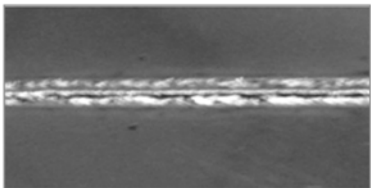
	Positive surface of welded joint	Back surface of welded joint
Welding parameters 1; $P=2\,000\text{ W}$, $v=1.5\text{ m/min}$, $E=800\text{ J/cm}$	 Width of weld: 3.00 mm	 Width of weld: 1.80 mm
Welding parameters 2; $P=2\,500\text{ W}$, $v=1.875\text{ m/min}$, $E=800\text{ J/cm}$	 Width of weld: 2.85 mm	 Width of weld: 1.45 mm

Fig.2 Welded joint appearance of positive and back surface of laser beam welding

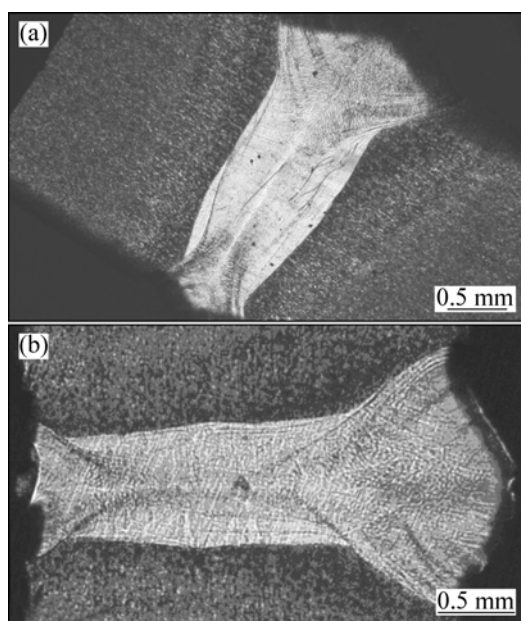


Fig.3 Macrostructures of cross-sections in laser beam welding performed at: (a) Parameters 1; (b) Parameters 2

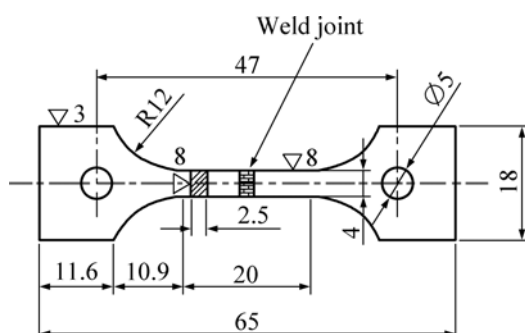


Fig.4 Dimensions of tensile specimens (Unit: mm)

were etched with (1%–3%)HF+(4%–6%)HNO₃+H₂O (volume fraction) solution. The specimens for XRD analysis were the longitudinal section specimens intercepted along the center of the welded joint, so the analysis surface was located in welded joint completely.

3 Results and discussion

3.1 Microstructure and properties of as-welded joints

The microstructure of the central part in as-welded joint is shown in Fig.5. The XRD patterns of the center of the longitudinal section of the as-welded joint are shown in Fig.6, which demonstrated that the center of the weld is mainly composed of β/B_2 phase. The weld zone was difficult to be etched compared to HAZ and the base metal, moreover no obvious multiphase structure was seen. The results of room-temperature and high temperature tensile properties of the as-welded joints are listed in Table 3. The room-temperature tensile strength of the joints is basically comparable to that of the base metal and the tensile ductility of the joints achieves 62% of that of the base metal. When the joints were transversely tensed at 650°C, the tensile strength was at a range of 650–716 MPa, but the tensile ductility only achieved 1.88%–2.25%. The rupture all occurred in the weld. Thus the β/B_2 phase of welded joint obtained by the laser beam welding was unstable at high temperature. The plasticity at 650 °C was obviously insufficient.

3.2 Microstructure and mechanical properties of joints after heat treatment

The microstructures of the joints processed with furnace cooling and air cooling after heat treatment at

980 °C for 1.5 h are shown in Fig.7. The XRD patterns of the base metal and the longitudinal section of the weld after heat treatment are shown in Fig.8. In the joints after furnace cooling, the microstructure of the base metal presented equiaxed grains primarily, but the white massive microstructure was reduced. The XRD analysis indicated that the base metal after furnace cooling was primarily $O+\alpha_2$ phase, and a few B_2 phase. However, after the furnace cooling at 980 °C for the weld zone, the columnar β/B_2 phase transformed to lamellar structure.

The XRD analysis showed that it mainly consisted of $O+\alpha_2$ phases. In the joints after air cooling, the microstructure of the base metal basically did not change, while the columnar β/B_2 phase transformed to lamellar structure on the weld zone, which consisted of $O+\alpha_2+B_2$ phases.

The properties of the joints at room temperature and high temperature after heat treatment are shown in Table 4. The room-temperature tensile strength and ductility of the joints were reduced after the heat treatment compared

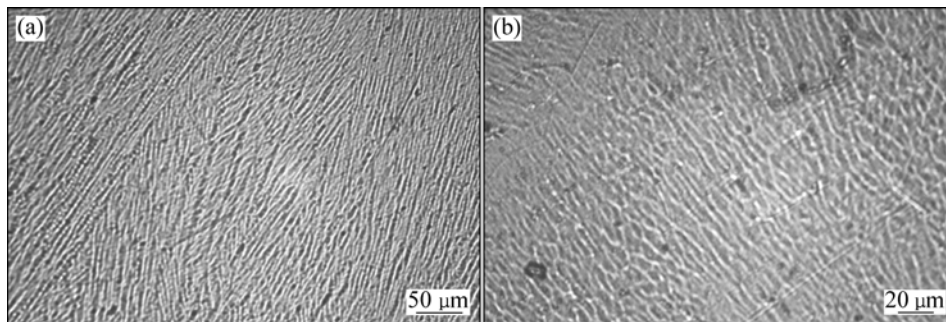


Fig.5 Microstructures of central part in as-welded joint performed at: (a) Parameters 1; (b) Parameters 2

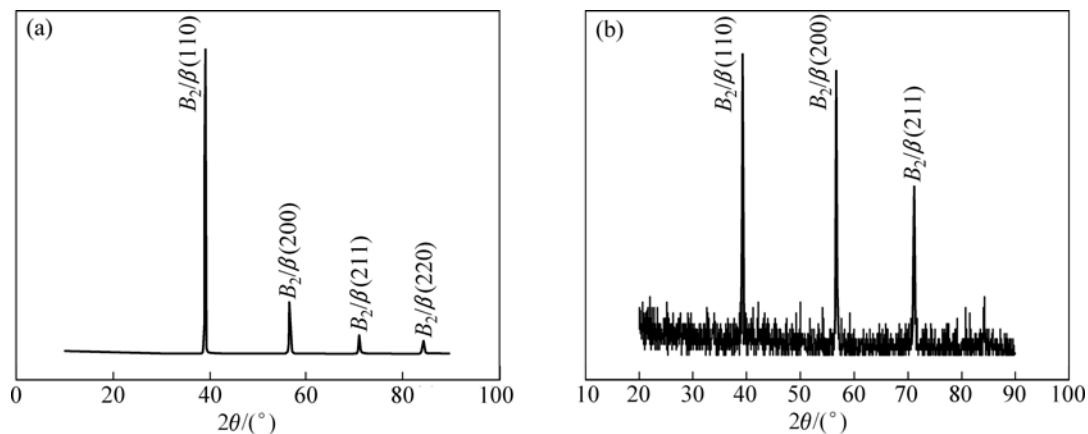


Fig.6 XRD patterns of longitudinal section in as-welded joint performed at: (a) Parameters 1; (b) Parameters 2

Table 3 Mechanical properties of as-welded joints

Temperature of transverse tensile tests	Welding condition	σ_b /MPa	$\sigma_{0.2}$ /MPa	δ /%	Fracture position
Room temperature	2 000 W, 1.5 m/min, $E=800$ J/cm	918.75	725.00	25.75	Weld metal: two samples Base metal: two samples
	2 500 W, 1.875 m/min, $E=800$ J/cm	886.25	760.00	24.75	Base metal
650 °C	2 000 W, 1.5 m/min, $E=800$ J/cm	651.25		2.25	Weld metal
	2 500 W, 1.875 m/min, $E=800$ J/cm	716.25		1.88	Weld metal

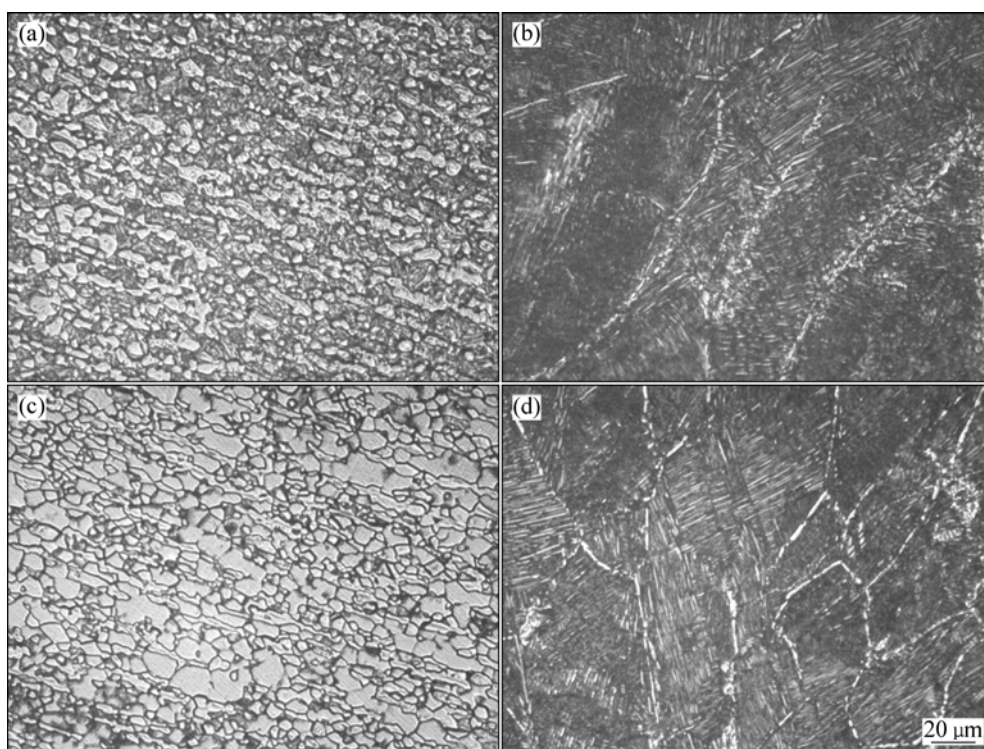


Fig.7 Microstructures of joints after heat treatment: (a) Base metal zone after furnace cooling; (b) Weld zone after furnace cooling; (c) Base metal zone after air cooling; (d) Weld zone after air cooling

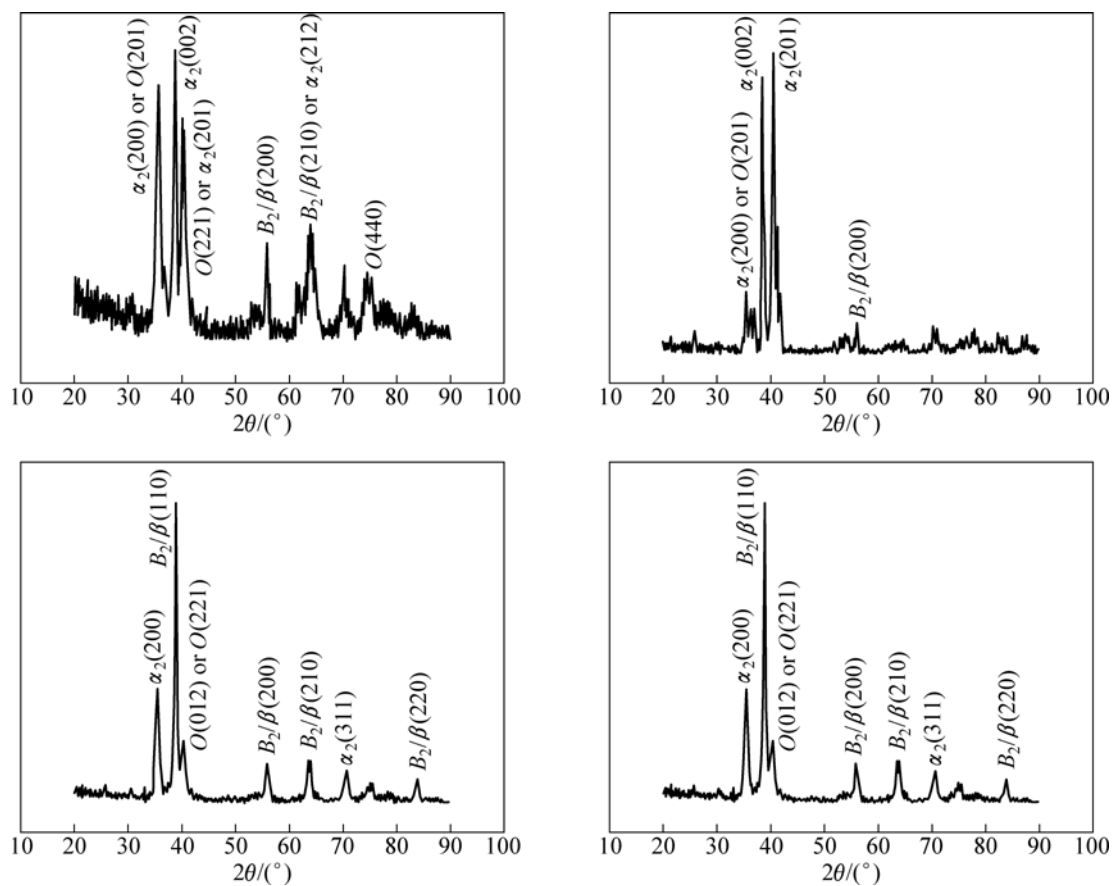


Fig.8 XRD patterns of base metal zone and weld zone after heat treatment: (a) Base metal processed with furnace cooling; (b) Weld zone processed with furnace cooling; (c) Base metal processed with air cooling; (d) Weld zone processed with air cooling

Table 4 Mechanical properties of joints after heat treatment

Temperature of transverse tensile tests	Heat treatment condition	Welding condition	σ_b /MPa	$\sigma_{0.2}$ /MPa	δ /%	Fracture position	
Room temperature	980 °C for 1.5 h, furnace cooling	2 000 W, 1.5 m/min, $E=800$ J/cm	630.00	465.00	10.00	HAZ	
		2 500 W, 1.875 m/min, $E=800$ J/cm	602.50	458.75	6.88	Weld metal	
	980 °C for 1.5 h, air cooling	2 000 W, 1.5 m/min, $E=800$ J/cm	792.50	680.00	8.00	Weld metal	
		2 500 W, 1.875 m/min, $E=800$ J/cm	788.75	656.25	9.13	Weld metal	
	650 °C	980 °C for 1.5 h, furnace cooling	2 000 W, 5 m/min, $E=800$ J/cm	401.25	—	46.50	Base metal
			2 500 W, 1.875 m/min, $E=800$ J/cm	392.50	—	48.00	Base metal: 3 samples Weld metal: 1 sample
980 °C for 1.5 h, air cooling		2 000 W, 1.5 m/min, $E=800$ J/cm	747.50	—	5.50	Weld metal	
		2 500 W, 1.875 m/min, $E=800$ J/cm	703.75	—	7.88	Weld metal	

with those in as-welded condition; therefore, rupture occurred in the weld and HAZ. The tensile strength of joints at room temperature after furnace cooling was 600–630 MPa, and the tensile ductility was 6.88%–10.00%. The tensile strength of joints at room-temperature after air cooling was 788–792 MPa, and the tensile ductility was 8.00%–9.13%.

After furnace cooling, the joints were tensed at 650 °C. The tensile strength was reduced to about 400 MPa, but the plasticity was improved enormously, the tensile ductility achieved above 40%, and the rupture occurred in the base metal. However, after the joints were air cooled and tensed at 650 °C, the tensile strength was about 703–747 MPa, which is comparable to that of the as-welded joints, the strength achieved 89% that of the base material, the plasticity was improved, and the tensile ductility achieved above 5%.

3.3 Discussion

The results of microstructure investigations and properties tests indicated that by laser beam welding, the β/B_2 phase of Ti-23Al-17Nb alloy did not transform at high temperature which were retained to the room temperature. The weld was basically composed of β/B_2 unstable phase at room temperature. Near the weld zone,

the HAZ was the field that the maximum temperature was over 980 °C. In the HAZ fields that the maximum temperature was between 980 °C and β phase transition temperature, equiaxed crystal of the base metal was basically preserved. However, the proportion of α_2 , B_2 and O changed, α_2 phase was reduced while B_2 phase increased. On the other hand, in the fields that the maximum temperature was over β phase transition temperature, the alloy was basically composed of β/B_2 unstable phase after cooling, so the base metal, HAZ and weld metal of the as-welded joints were composed of $\alpha_2+\beta_2+O$ equiaxed grains, $(\alpha_2+\beta_2+O)/(\beta/B_2)$ equiaxed grains and β/B_2 columnar grains, respectively. When the transverse tensile tests of joints were carried out at room temperature, the orientation of columnar crystal made it difficult to deform, so the deformation mainly concentrated on the base metal with equiaxed crystal. The gauge length of the transverse tensile specimens was 20 mm, the length of deformable base metal in gauge length was about 12 mm besides the weld zone (3–4 mm) and its affected zone. Therefore, when the transverse tensile tests of joints were carried out at room temperature, the tensile strength was comparable to that of the base metal, the tensile ductility achieved about 60% that of the base metal.

When the as-welded joints were transversely tensed at 650 °C, Ti-23Al-17Nb alloy was in O phase zone according to Ti₃Al-Nb pseudo binary phase diagram[19]. The unstable β/B_2 phase would transform to the microstructure mainly composed of O phase, which also preserves the columnar crystal appearance of the weld metal. After the as-welded joints were tensed at 650 °C, the microstructure observed at room temperature is shown in Fig.9. The weld metal was composed of coarse columnar crystal structure of O single-phase which was easily fractured along the boundary of the columnar crystal grain when the metal was transversely tensed. Fig.10 shows the fractograph of the metal tensed at 650 °C. The plasticity was lower; the tensile ductility was

only 1.88%–2.25%.

When processed with heat treatment at 980 °C, Ti-23Al-17Nb alloy was in α_2+B_2+O three-phase zone at this temperature range. The original unstable β/B_2 phase would transform to α_2+B_2+O three-phase structure when the welded joint was holding at this temperature, and B_2 phase would further transform to α_2+O phase during furnace cooling. However, the microstructure at 980 °C was basically preserved after air cooling. Because the original β/B_2 grain of the weld metal was coarser columnar crystal compared with fine equiaxed structure of the base metal, the lamellar structure which was formed during $\beta/B_2 \rightarrow \alpha_2+B_2+O$ phase transformation was coarser, and certain orientation inheritance existed during phase transformation. Therefore, after the heat treatment, tensile strength and tensile ductility of the welded joint at room temperature were reduced compared to those of the base metal and the as-welded joint. However, when the joint was tensed at 650 °C, its microstructure was three-phase lamellar structures; the plasticity was improved compared with coarse columnar crystal structure of single phase in the as-welded joint at 650 °C. Consequently, the ductility of the joints after heat treatment was improved when the joints were tensed at high temperature.

4 Conclusions

1) When Ti-23Al-17Nb alloy laser beam welding joint in as-welded condition was transversely tensed at room temperature, its tensile strength was 886–918 MPa, which was comparable to that of the base metal. The tensile ductility was about 25%, which achieved about 60% of that of the base metal. When the joint was transversely tensed at 650 °C, the tensile strength was 651–716 MPa, the tensile ductility was 1.88%–2.25%, and the rupture occurred in the weld.

2) After being processed with the furnace cooling at 980 °C for 1.5 h, the microstructures of the base metal and the weld metal were mainly $O+\alpha_2$ phase, and the equiaxed crystal of the base metal was basically preserved, but the weld zone presented lamellar structure. Tensile properties of the joints after the heat treatment at room-temperature were reduced compared with those in as-welded condition. The tensile strength was 602–630 MPa and the tensile ductility was 6.88%–10.00%. When the joints were transversely tensed at 650 °C, the tensile strength was only 392–401 MPa, but the tensile ductility achieved above 40%.

3) After being processed with the air cooling at 980 °C for 1.5 h, the microstructure of the base metal did not change, α_2+B_2+O three-phase structure and equiaxed crystal were preserved, and the weld metal showed α_2+B_2+O three-phase lamellar structure. The room-

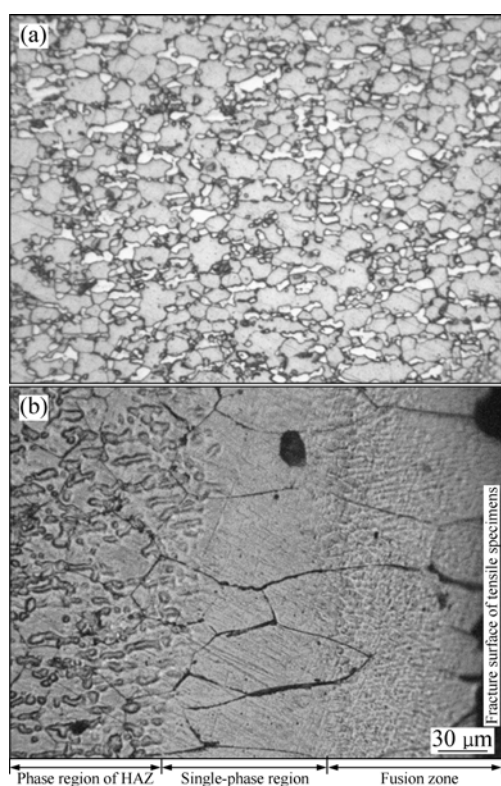


Fig.9 Microstructures of as-welded joints after high temperature tensile tests at 650 °C: (a) Base metal; (b) HAZ and weld zone

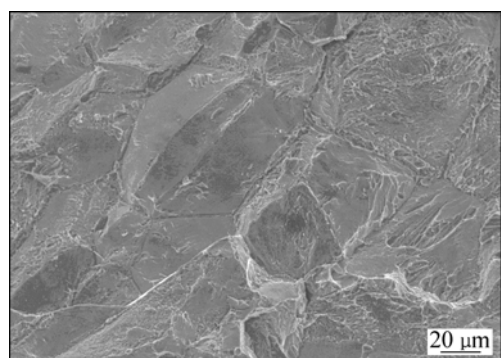


Fig.10 Fractograph of as-welded joints after tensile tests at 650 °C

temperature tensile properties of the joints after the heat treatment were appreciably reduced compared with that in as-welded condition, but the tensile strength was higher than that of the joints after furnace cooling. The tensile strength was 789–792 MPa, and the tensile ductility achieved 8.00%–9.13%. When the joint was transversely tensed at 650 °C, the tensile strength achieved 704–747 MPa, and the tensile ductility was 5.50%–7.88%, which was higher than that in as-welded condition.

References

- [1] YE Heng-qiang. Recent developments in high temperature intermetallics research in China [J]. *Intermetallics*, 2000, 8(5/6): 503–509.
- [2] SONG Dan, DING Jin-jun, WANG Yan-dong. Influence of alloy element (Nb, Mo, V) on microstructure of Ti₃Al base alloys [J]. *Acta Metall*, 1996, 9(2): 85–88.
- [3] ZHANG J W, LI S Q, ZOU D X, MA W Q, ZHONG Z Y. Processing and microstructure control of ($\alpha_2+\beta+O$) alloy sheet in Ti-Al-Nb system [J]. *Intermetallics*, 2000, 8(5/6): 699–702.
- [4] DING H, SONG D, ZHANG C B, CUI J Z. Superplastic behavior of α/β -forged Ti₃Al-Nb alloy [J]. *Mater Sci Eng A*, 2000, 281(1/2): 248–252.
- [5] DJANARTHANY S, VIALA J C, BOUIX J. An overview of monolithic titanium aluminide based on Ti₃Al and TiAl [J]. *Mater Chem Phys*, 2001, 72: 301–319.
- [6] WANG Guo-qing, WU Ai-ping, ZOU Gui-sheng, ZHAO Yue, CHEN Qiang, REN Jia-lie. Bending properties and fracture behavior of Ti-23Al-17Nb alloy laser beam welding joints [J]. *Tsinghua Science and Technology*, 2009, 14(3): 293–299.
- [7] FENG Ji-cai, WU Hui-qiang, HE Jing-shan, ZHANG Bin-gang. Microstructure evolution of electron beam welded Ti₃Al-Nb joint [J]. *Materials Characterization*, 2005, 54: 99–105.
- [8] HE P, FENG J C, ZHOU H. Microstructure and strength of brazed joints of Ti₃Al-base alloy with different filler metals [J]. *Materials Characterization*, 2005, 54: 338–346.
- [9] THREADGILL P L. The prospects for joining titanium aluminides [J]. *Mater Sci Eng A*, 1995, 192/193: 640–646.
- [10] BAESLACK III W A, MASCORELLA T J, KELLY T J. Weldability of a titanium aluminide [J]. *Welding Journal*, 1989, 68(12): 483s–498s.
- [11] BAESLACK III W A, PILLIPS D, SCARR G K. Characterization of the weld heat-affected zone in a alpha-two titanium aluminide [J]. *Materials Characterization*, 1992, 28: 61–73.
- [12] CIESLAK M J, HEADLEY T J, BAESLACK W A III. Effect of thermal processing on the microstructure of Ti-26Al-11Nb: Applications to fusion welding [J]. *Metall Trans A*, 1990, 21A(5): 1273–1286.
- [13] BAESLACK K W A III, BRODERICK T. Effect of cooling rate on the structure and hardness of a Ti-26Al-10Nb-3V-1Mo titanium aluminide [J]. *Scripta Metall Mater*, 1990, 24(2): 319–324.
- [14] DAVID S A, HORTON J A, GOODWIN G M, PHILLIPS D H, REED R W. Weld ability and microstructure of a titanium aluminide [J]. *Welding Journal*, 1990, 69(4): 133s–140s.
- [15] MARTIN G S, ALBRIGHT C E, JONES T A. An evaluation of CO₂ laser beam welding on a Ti₃Al-Nb alloy [J]. *Welding Journal*, 1995, 74(2): 77s–82s.
- [16] WU Ai-ping, ZOU Gui-sheng, REN Jia-lie, ZHANG Hong-jun, WANG Guo-qing, LIU Xin, XIE Mei-rong. Microstructure and mechanical properties of Ti-24Al-17Nb (at.%) laser beam welding joints [J]. *Intermetallics*, 2002, 10(7): 647–652.
- [17] THREADGILL P L. Metallurgical aspects of joining titanium aluminide-alloys//[C] *Proc Int Symp On Intermetallic Compounds (JIMIS-6)*. Sendai, apan, 1991: 1021–1025.
- [18] WANG Guo-qing, ZHAO Yue, WU Ai-ping, ZOU Gui-sheng, REN Jia-lie. Microstructure and high-temperature tensile properties of Ti₃Al alloys laser welding joint [J]. *The Chinese Journal of Nonferrous Metals*, 2007, 17(11): 1803–1807. (in Chinese)
- [19] CHEN Guo-liang, LIN Jun-pin. Physical metallurgy of the ordered intermetallic structural materials [M]. Beijing: Metallurgical Industry Press, 1999: 271–275. (in Chinese)

(Edited by FANG Jing-hua)